



# Düzce University Journal of Science & Technology

Research Article

## Comparison of The Output Power of a Micro Hydroelectric Power Plant with Different PID Control Structures

Tuğba AYDIN KART<sup>a-b\*</sup>, Ahmet AKTAŞ<sup>a</sup>, Ömür BINARBAŞI<sup>b</sup>, Batuhan ŞENLEN<sup>a-b</sup>,

<sup>a</sup> Department of Energy Systems Engineering, Faculty of Technology, Gazi University, Ankara, Türkiye

<sup>b</sup> Department of R&D and Innovation, Türkiye Electromechanic Industry Corporation, Ankara, Türkiye

\* Corresponding author's e-mail address: tugba.aydin@temsan.gov.tr

DOI: 10.29130/dubited.1568330

### ABSTRACT

In this study, a micro-hydroelectric power plant that produces energy from the water taken from the Ulutan Dam and sends it to the treatment plant for drinking water purposes was examined. The control and command system of the grid-connected micro HPP (Hydroelectric Power Plant) is implemented using Siemens S7 1200 PLC. After synchronization of the system with the grid, two different control software are loaded sequentially. The first one is a PID controller created for the position control of the turbine guide vane, while the second software is the power set PID controller. In the study, the data regarding the position of the guide vane, flow rate, pressure, and active power, which were obtained from the turbine control system, are analyzed. Both PID controls reached the maximum active power value of 137 kW. However, while the guide vane PID controller maintained the maximum power value, the power set PID controller could not stabilize the system. The power set PID controller could not maintain the stabilization of the system, the turbine took in more water to provide the power, the flow rate increased over time and the pressure decreased. The power of this system also decreased from 137 kW to 105 kW. Since the aim was to achieve maximum power and stable operation, it was concluded that the guide vane PID control block was more efficient.

Through this project, an unused water source was evaluated, contributing to the national economy, and providing valuable experience and knowledge for the control and command systems to be used in the installation or rehabilitation of a micro-hydroelectric power plant.

**Keywords:** Micro HPP, PID Control, PLC, guide vane, power adjustment

## Farklı PID Kontrol Yapıları İle Bir Mikro Hidroelektrik Santral Çıkış Gücünün Karşılaştırılması

### ÖZ

Bu çalışmada Ulutan Barajından arıtma tesisine içme suyu maksadıyla alınan sular ile enerji üretimi yapan bir mikro hidroelektrik santral incelenmiştir. Şebekeye bağlı olan Mikro HES (Hidroelektrik Santral)'in kontrol ve kumanda sistemi Siemens S7 1200 PLC ile gerçekleştirilmiştir. Sistemin şebekeye senkronizasyonu sonrası iki farklı kontrol yazılımı sırasıyla yüklenmiştir. Bunlardan ilki türbin ayar kanadının pozisyon kontrolü için oluşturulan PID kontrolörü, ikinci yazılım olarak güç set PID kontrolörüdür. Çalışmada; türbin kontrol sisteminden alınan ve kontrol edilen ayar kanadı pozisyonu, debi, basınç ve aktif güç verileri analiz edilmiştir. İki farklı PID

kontrolü de maksimum aktif güç değeri olan 137 kW'a ulaşmış fakat ayar kanadı PID kontrolörü maksimum güç değerini korurken güç set PID kontrolörü sistemin stabilizasyonunu koruyamamış gücü sağlayabilmek için türbine daha çok su almış, debi zamanla artmış, basınç azalmıştır. Bu sebeple sistemin gücü de 137 kW değerinden 105 kW değerine kadar düşmüştür. Sistemin maksimum gücü elde edebilmesi ve stabil çalışması istendiğinden bu koşulları sağlayan ayar kanadı PID kontrol bloğunun daha verimli kontrol bloğu olduğu sonucuna varılmıştır. Bu projeye enerjisinden yararlanılmayan su kaynağı değerlendirilip ülkemizin milli servetine katkısı sağlanmış, bir mikro hidroelektrik santral kurulumunda veya rehabilitasyonu esnasında kontrol kumanda sistemlerinde kullanılması için tecrübe bilgi birikimi aktarılmıştır.

**Anahtar Kelimeler:** Mikro HES, PID Kontrol, PLC, ayar kanadı, güç ayarı

## **I. INTRODUCTION**

The growth of the global population and the increasing prevalence of technological products have significantly raised the energy demand. Fossil fuels meet a large percentage of this energy need. When the general energy use denominator of the world population is examined, the most used energy source is fossil fuels (oil, coal, natural gas) with 76% in the first place, renewable resources (solar, wind, biofuel, etc.) in the second place with 20%, and nuclear in the third place with 4% energy usage comes [1]. Usage percentages are shown graphically in Figure 1.

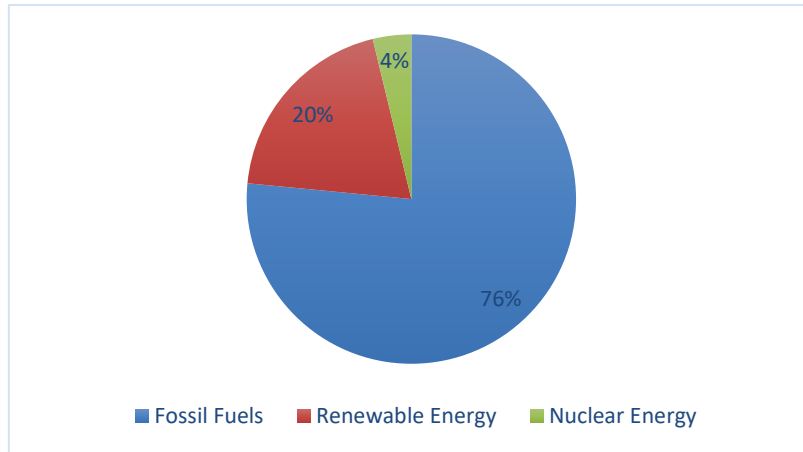


**Figure 1.** Global Energy Consumption by Source in 2023

As a result of the percentage of use of fossil fuels, global warming is accelerating day by day, and to prevent climate change, countries are taking some measures to reduce the use of fuels that create their carbon footprint and turn to renewable resources.

Türkiye is a country that is very abundant in terms of renewable energy. Hydroelectric energy ranks first among renewable resources with its high energy reserve feature. According to the data of the Ministry of Energy, as of the end of June 2024, our country's installed power reached 110,518 MW, and hydraulic energy ranked first with 29.1% in the distribution of our installed power by resources [2].

To evaluate the potential of HEPP (Hydroelectric Power Plant), small-scale HEPPs that are easy to install and do not harm the environment, which will provide an advantage to rural areas where electricity transportation is difficult, should be evaluated as well as large HEPPs. The power classification of small HEPPs varies in the literature. In general, HEPPs between 2MW and 25MW are considered small-scale hydroelectric power plants [3].

*Table 1. Small-Scale HPP Classification*

	Capacity
Pico-Hydro	< 10 kW
Micro-Hydro	< 500 kW
Mini -Hydro	< 2 MW

## **II. LITERATURE REVIEW**

This chapter presents a comprehensive review of the literature on the control of small HEPP power plants. One of the most important parameters when controlling a HEPP is that the frequency and voltage are stable. A lot of research has been done regarding this. As an example; Nikhila Sanampudi and his colleague emphasized the 10,000 MW micro-HPP potential in India in their study. They developed an electronic load control design to maintain frequency and voltage stability under varying loads and found that it could be used efficiently and effectively [4]. Suhas and his colleagues conducted a comprehensive literature review on load frequency control in micro-hydroelectric power plants. They presented a fuzzy logic-based controller design to manage the entire operation of the production unit. The role of the fuzzy logic-based controller was to regulate the plant's frequency output despite varying user loads and to limit the waste of available water. They developed a simulation model of a micro-HPP using blocks available in MATLAB SIMPOWER and were able to keep the frequency stable under varying user loads [5]. Oğuz, A. Kaysal, and K. Kaysal simulated the dynamic behavior of load-frequency control in the Adıgüzel HPP under varying loads using MATLAB/Simulink and SimPowerSystems Toolbox. According to the frequency-voltage curve obtained, they found that by maintaining the excitation circuit voltage constant, oscillations in frequency were due solely to changes in active power, which resulted in oscillations in terminal voltage [6]. In their study, Öztürk, Özdemir and Cebeci examined the frequency and voltage changes in inductive and ohmic load situations in small and very low-power HEPPs by providing PID control with PLC through an experimental set with a synchronous generator-driven by a direct current motor [7]. In another study, Özkan and his colleagues designed a hydroelectric power plant prototype as educational material, controlling it via PLC. Using a Pelton turbine, they observed the rotational speed and the voltage produced [8].

Several studies have also been published in the literature comparing two distinct control methods. For instance, previous studies have shown that: Dalcalı and colleagues designed a microcontroller-based governor system (speed regulator), comparing the generator's output frequency with the microcontroller and adjusting the amount of water through the guide vane based on the result. By using microcontrollers, mechanical losses and reaction time have been minimized, resulting in a more cost-effective control system compared to PLC [9]. In a study conducted in 2022, Ulu and Altinkaya used both conventional Proportional Integral Derivative (PID) control and Artificial Neural Networks (ANN)-based PID control methods for the control system of a micro-HPP prototype. They found that the ANN-based PID provided better results than the conventional PID in terms of settling time, frequency and voltage overshoots [10].

One of the key parameters influencing the production potential of a hydroelectric power plant is the rainfall potential. In this context, Chatchophang and colleagues, noting that the water flow and height in small hydroelectric power plants change seasonally, proposed that the turbine's torque-speed characteristics must be adjusted for the generator to operate at variable speeds to achieve maximum power. They developed an algorithm for variable speed control and maximum power point tracking of a Permanent Magnet Synchronous Generator (PMSG) and applied it in Thailand. To simulate the turbine's torque-speed characteristics, they used a servo drive-controlled permanent magnet synchronous motor, and the experimental results validated their proposed speed control algorithm [11].

Halil Kurt, who aimed to test the software with varying numbers of turbines, examined the Kayaboğazi Dam in Kütahya and compared the energy potential of three turbines planned to exist with one turbine by using PLC with a fuzzy logic algorithm for commissioning and decommissioning the turbines to benefit from energy production at an optimal level and compared the investment costs [12].

### **III. MATERIAL AND METHOD**

In this study, electricity generation was carried out by utilizing water taken from the Ulutan Dam, located in the Black Sea Region within the borders of Zonguldak, for drinking purposes. The control and automation of the 200 kW micro-hydro power plant (HPP), connected to the grid, were implemented using Siemens S7-1200 PLC modules and a Human-Machine Interface (HMI) SCADA screen. The control system of the designed micro-HPP was operated using two different software programs. After the synchronization of the system with the grid, the first software, the guide vane PID control, was tested. The opening percentage of the turbine's guide vane was manually entered via the SCADA screen, and the amount of water passing through the turbine ( $\text{m}^3/\text{h}$ ) was controlled, allowing the system to operate. The data were analyzed, and graphs were generated.



*Figure 2. Overview of Micro Hydro Power Unit*

The second software, the power set PID control, was then tested. The desired active power value was entered via the SCADA screen, and the guide vane opening percentage was automatically adjusted by the PID control block to achieve the desired power. The data were analyzed and graphed.

The active power values produced at different flow and pressure levels were compared between the two different software programs.



**Figure 3.** Control and Command SCADA panel

Throughout the 24-hour operation of the system, various data were monitored from the SCADA screen, such as current, voltage, frequency, power, flow rate, guide vane opening, pressure before and after the inlet valve, turbine bearing temperatures, generator bearing temperature, and the oil temperature of the hydraulic unit. The values recorded every second were used as reference data in this study. The data collected from the field were categorized into digital and analog signals, as presented in Table 2.

**Table 2.** Data Collected from The Field

Equipment	Explanation	Digital Input	Digital Output	Analog Input	Analog Output
Generator	• Acceleration Sensor	✓	X	X	X
PLC Panel	• Emergency Stop	✓	X	X	X
MCC Panel (Motion Control Chart)	• Grid Busbar Energized	✓	X	X	X
	• Load Disconnecter Active	✓	X	X	X
	• Generator (TMS) Thermal Magnetic Switch Active	✓	X	X	X
Generator	• Breaker Active	✓	X	X	X
	• Generator TMS Active	✓	X	X	X
Bypass Valve	• Thermal Fault	✓	X	X	X
	• Open	✓	✓	X	X
	• Close	✓	✓	X	X
Inlet Valve	• Thermal Fault	✓	X	X	X
	• Open	✓	✓	X	X
	• Close	✓	✓	X	X

**Table 2 (cont).** Data Collected from the field

Hydraulic Pump	• Thermal Fault	✓	x	x	x
	• Running	✓	✓	x	x
Stand-by motor	• Thermal Fault	✓	x	x	x
	• Running	✓	x	x	x
Hydraulic Unit	• Oil pressure emergency	✓	x	x	x
	• Oil filter unclean	✓	x	x	x
	• Oil-level low	✓	x	x	x
	• Hydraulic oil pressure	x	x	✓	x
Excitation System	• AVR Active	x	✓	x	x
	• AVR Passive	x	✓	x	x
	• Excitation Trip	x	✓	x	x
Safety System	• PLC Emergency stop output	x	✓	x	x
Generator	• Breaker Active	x	✓	x	x
	• Breaker Low Voltage	x	✓	x	x
Protective Relay	• Generator Frequency	x	x	✓	x
	• Active Power	x	x	✓	x
Ambient Temperature		x	x	✓	x
Penstock Pipe	• Pressure before Inlet valve	x	x	✓	x
	• Pressure after Inlet valve	x	x	✓	x
Turbine Guide Vane Position		x	x	✓	x
Generator	• Bearing Temperature	x	x	✓	x
	• Winding Temperature	x	x	✓	x
Turbine	• Bearing Temperature	x	x	✓	x
Flow Rate		x	x	✓	x

When calculating the total capacity of a hydroelectric power plant, important parameters must be considered. The two most significant parameters are flow rate and head [13]. The hydraulic power produced is proportional to the flow rate and head, as shown by Equation (1);

$$P_{hydraulic\ power} = \rho \cdot g \cdot H_{net} \cdot Q \cdot \eta \quad (1)$$

Where,  $\rho$  (kg/m<sup>3</sup>) is the specific gravity of water,  $g$  (m/s<sup>2</sup>) is the gravitational acceleration,  $H_{net}$  (m) is the net head,  $Q$  (m<sup>3</sup>/s) is the flow rate,  $\eta$  is efficiency of turbine [14].



The selection of the generator is based on the hydraulic power obtained from the turbine, as expressed in Equation (2);

$$P_{active\ power} = S \times \cos\theta \quad (2)$$

In the equation,  $S$  (kVA) is the apparent power,  $\cos\theta$  is the power factor [15].

The generator frequency must be within acceptable values so that the generator terminal voltages can be synchronized with the grid in HEPPs. The values that can be considered suitable for the stable operation of the system are the frequency of 50 Hz (+/-0.2) and the voltage level of 400V (+/-20) [16].

The task of the control system in hydroelectric power plants is to keep the generator frequency and terminal voltages within acceptable limits and to ensure power balance by controlling active and reactive power [4]. For this purpose, PLC and microcontroller-based systems are used.

The Equation (3) and Equation (4) are used to keep the generator frequency and terminal voltage at a constant value.

$$f = n \times P / 120 \quad (3)$$

Where,  $f$  (Hz) is the frequency of the voltage generated by the generator,  $n$  (rpm) is the rotational speed of the generator and  $P$  is the number of poles [4].

Since the frequency of the generator's output voltage is directly proportional to its rotation speed, frequency control is achieved by changing the speed of the turbine that rotates the generator shaft. Turbine speed depends on the amount of water passing through the turbine. Depending on the turbine type, the turbine speed is controlled by increasing/decreasing the turbine adjustment guide vane or nozzle position and the amount of water passing through.

$$E = K \cdot \varphi \cdot \omega \quad (4)$$

In equation (4),  $E$  is the induced voltage,  $K$  is the constant coefficient,  $\varphi$  is the magnetic flux created by the excitation winding, and  $\omega$  is the angular velocity.

According to the Equation (4), the generator terminal voltages can be controlled by changing the  $\varphi$  magnetic flux (generator excitation flux) and  $\omega$  rotation speed. In systems synchronized with the grid, since the frequency must remain constant, voltage control is achieved using an Automatic Voltage Regulator (AVR). The output voltages of the generator are measured, and the excitation current is increased or decreased accordingly to bring the generator's terminal voltages to nominal values [16].

Micro-HPPs can operate either connected to the grid or independently. For grid-connected HPPs, after synchronization, the generator's frequency must match the grid frequency and remain stable. This requires the generator's rotational speed to remain at synchronous speed [17].

The mechanical power on the turbine shaft is converted into electrical power via the generator rotor. The active power produced by the generator is proportional to the turbine shaft power. In grid-connected systems, the frequency and voltage of the generator remain constant in synchronized conditions. Angular speed is constant in the shaft power formula given in Equation (5). To change the shaft power, it is necessary to change the mechanical torque. The mechanical torque change depends on the flow rate and pressure values. Therefore, after synchronization, the turbine adjustment guide vane position affects the generated active power value. The amount of water entering the turbine is controlled by the turbine's adjustment guide vane. In case of high-power demand, the adjustment guide vane will be opened,

allowing a large amount of water to pass to the turbine; and for less power demand, the adjustment guide vane will be closed, allowing less water passage to the turbine.

$$P_{shaft\ power} = T \cdot \omega \quad (5)$$

Where,  $\omega$  (rad/s) is the angular velocity,  $T$  (Nm) is the turbine shaft torque and  $P$  is the power in Watts [18].

A banki-type turbine was selected based on flow rate and head in this study. The water flow to the turbine was controlled by the guide vane. The opening and closing movement of the mechanism is provided by the forward/backward movement of the hydraulic piston located on the adjustment guide vane. A 4-20mA sensor is placed on the hydraulic piston to detect its movement.

The data obtained were evaluated in PLC-based software and controlled using PID control blocks.

As water passes through the adjustment vane, the generator begins to gain speed. Excitation is given to the generator when the speed of the generator is 90% or over. To stabilize the generator frequency within the acceptable range of 50 Hz (+/- 0.2), the instantaneous data received from the speed sensor is compared in the PID control block with the set value of 1500 revolutions, which is the number of revolutions corresponding to the 50 Hz, and stabilized and controlled.

After the system is synchronized, all conditions are now ready to generate electrical energy from the system.

The amount of water passing through the turbine was controlled by using two different PID control blocks in the system. The two different PID control blocks are as follows:

- 1- Guide Vane PID Control
- 2- Power Set PID Control

## A. FUNCTION OF PID

The "proportional" in the name of PID refers to the current control error, the "integral" refers to the past control error, and the "derivative" refers to the predicted control error. It is controlled with these data. The PID algorithm serves as an (AVR) for micro-hydraulic systems [19]. PID brings the error between the reference value and the actual value to an acceptable value.

The PID algorithm works according to Equation (5) given below.

$$y = K_p \left[ (b \cdot w - x) + \frac{1}{T_1 \cdot s} (w - x) + \frac{T_D}{\alpha \cdot T_D \cdot s + 1} (c \cdot w - x) \right] \quad (5)$$

In this equation,  $y$  is the output value of the PID algorithm,  $K_p$  is the proportional gain,  $s$  is the Laplace operator,  $b$  is the proportional effect weight,  $w$  is the set point,  $x$  is the process value,  $T_1$  is the integral effect time,  $T_D$  is the derivative effect time,  $\alpha$  is the derivative delay coefficient,  $c$  is the derivative effect weight [20].

The situation where there is no derivative effect is considered PI control. The difference signal between the process value and the reference value is integrated over time. When the difference signal is zero, the integrator circuit will not receive a signal, as soon as the differential signal is zero, the integrator will not receive the circuit signal [21].

PID should be preferred in complex systems where a PI controller is not sufficient. If the PI controller system ensures a steady state, there is no need to add a differential controller. Two different PID controllers were tested in this study.



There are two PID parameter adjustment procedures in the Siemens S7-1200 PLC controller, which are described as pretuning and fine tuning. It includes the Chien-Hrones-Reswick method for pretuning and the Ziegler-Nichols method for fine tuning [20].

In practice, the PID parameters were automatically tuned by the PLC controller, and refinements were made through an iterative process of trial and error.

## **IV. RESULT AND DISCUSSION**

### **A. GUIDE VANE PID CONTROL**

Initially, the commissioning process was carried out with the guide vane position PID control block. As shown in Figure 4, the requested percentage of guide vane was entered as "Set Entry" on the SCADA screen. The current position information of the guide vane taken from the linear potentiometer and the requested opening amount of the guide vane were sent to the input part of the PID control block as a percentage value, and the system tried to stabilize at the requested opening percentage by evaluating the two data.

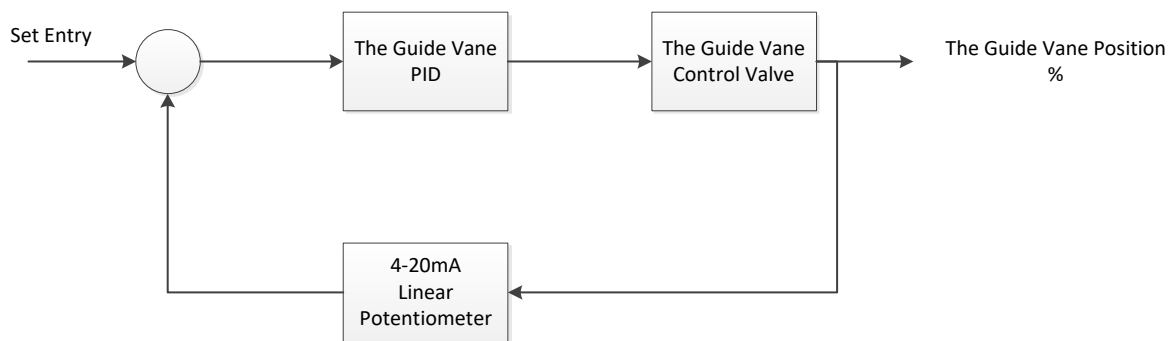


**Figure 4.** The Guide Vane PID Control Block Diagram

<input checked="" type="checkbox"/> Enable manual entry	
Proportional gain:	3.607911
Integral action time:	9.997746 s
Derivative action time:	4.668555E-1 s
Derivative delay coefficient:	0.1
Proportional action weighting:	0.8
Derivative action weighting:	0.0
Sampling time of PID algorithm:	1.000006 s

**Figure 5.** The Guide Vane PID Control Block Parameters

Before synchronization, the guide vane was opened to 43.41%, and in parallel, the flow rate reached up to 991.67 m<sup>3</sup>/h. Since a certain amount of water is supplied to the turbine to synchronize it with the network, the pressure and flow rate values in the graphs will start from 991.67 m<sup>3</sup>/h. Since a certain amount of water is supplied to the turbine to synchronize it with the grid, the pressure and flow rate values in the graphs will start from 991.67 m<sup>3</sup>/h.

Data was analyzed according to the guide vane position PID control block, active power, guide vane position, pressure and flow rate information. These data are graphed in Figures 6,7 and 8.

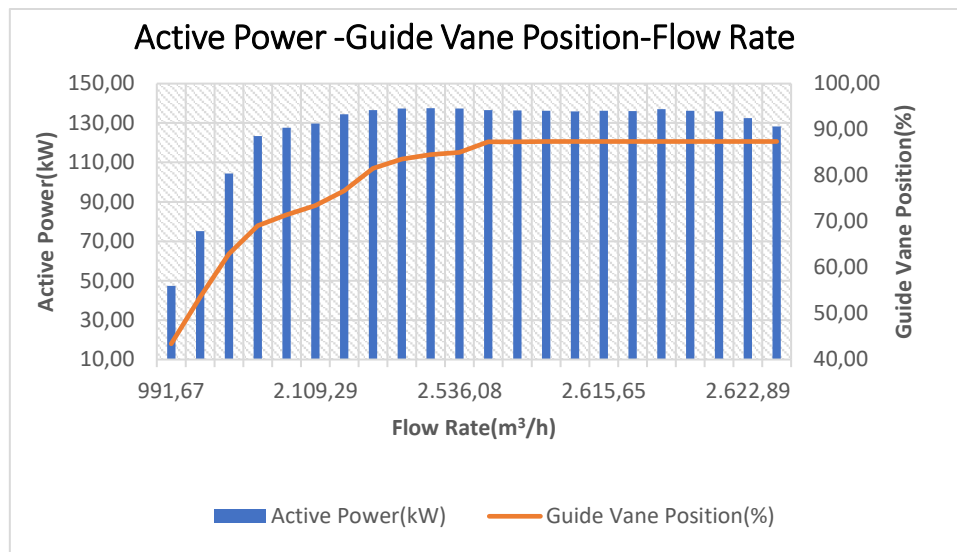


**Figure 6.** According to The Guide Vane PID Control Block; The Graph of The Active Power, Guide Vane Position and Flow Rate

The guide vane position has been increased by 10%, up to 90% clearance. Depending on the opening ratio of the guide vane, the flow rate increased accordingly. As shown in Figure 6, the flow rate starts to show a tendency to remain at a constant value after 81.58%. The highest flow rate (m³/h) is when the guide vane is open at 87.4%. The maximum flow rate was observed as 2,622.89 m³/h. The maximum value of the active power produced was observed as 137.57 kW when the guide vane was at 84.55%. When the guide vane position was 87.4%, 136 kW active power was produced, and the system tended to remain stable at this value.

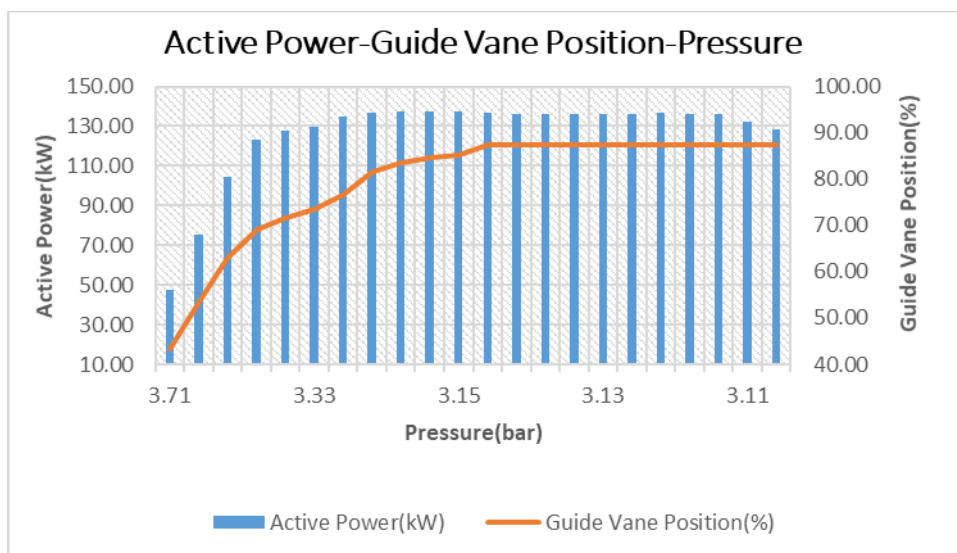


**Figure 7.** According to The Guide Vane PID Control Block; The Graph of The Active Power, Guide Vane Position and Pressure

As shown in Figure 7, the guide vane position has started to increase in percentage terms, and it has been observed that the pressure decreases regularly as the percentage of the guide vane position increases. When the guide vane position was 43.41%, the pressure was measured as 3.71 bar, and when

the guide vane position was 87.41%, the pressure was measured as 3.11 bar. At the highest active power value of 137.57 kW, the pressure was observed as 3.16 bar. Active power was measured as 128.29 kW at 3.11 bar, which is the moment when the pressure is lowest.

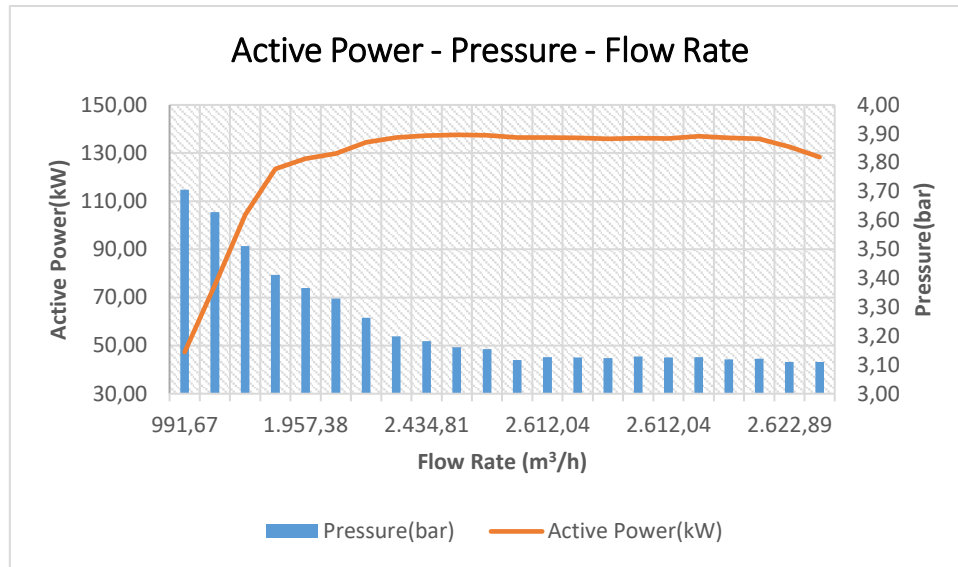


**Figure 8.** According to The Guide Vane PID Control Block; The Graph of The Active Power, Pressure and Flow Rate

According to Bernoulli's principle, the proportionality between the speed of the fluid and its pressure is inverse. Depending on the inverse proportionality, a decrease in the pressure in the section is observed as the speed of the fluid increases. Similarly, the pressure increases in the section where the speed decreases. It is observed in Figure 8, as the flow rate increases, the pressure tends to decrease, and when the flow rate tends to stabilize, the pressure also begins to stabilize. The highest active power was 137.57 kW, at this power value the flow rate was 2,499.91 m³/h and the pressure were measured as 3.16 bar.

## B. POWER SET PID CONTROL

In this section, the system is synchronized to the grid with the power set PID control block, which we mentioned as the second software. The requested power value was entered on the SCADA screen as shown in Figure 9. The current power and the requested Power are sent to the input of the PID control block and the control block tries to reach the requested power value by evaluating the two data. The Power PID block sends the output value to the input of the guide vane PID block, the guide vane stabilizes the system by activating the position of the guide vane control valve to reach the target power.

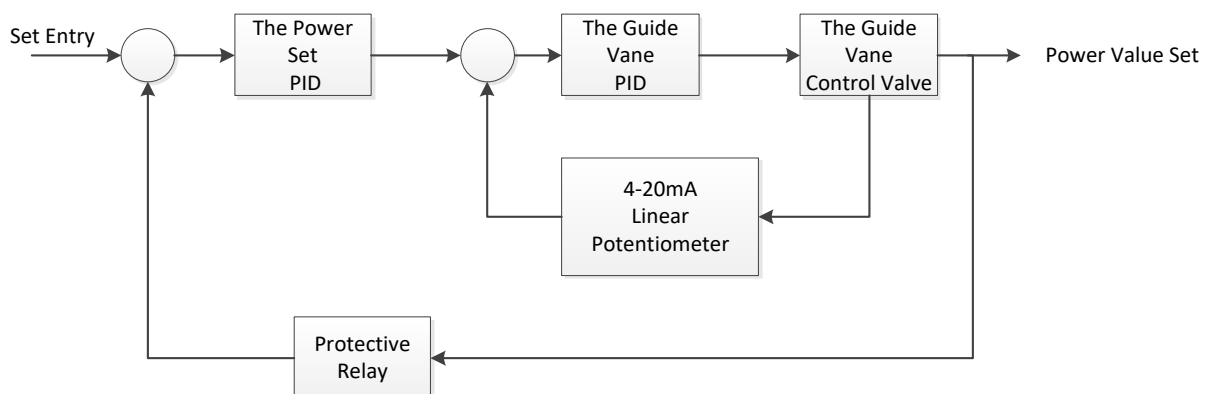


**Figure 9.** Power Set PID Control Block Diagram

☒ Enable manual entry

Proportional gain:

Integral action time:  s

Derivative action time:  s

Derivative delay coefficient:

Proportional action weighting:

Derivative action weighting:

Sampling time of PID algorithm:  s

**Figure 10.** Power Set PID Control Block Parameters

The same values (active power, guide vane position, pressure and flow rate) examined in the guide vane PID control block are shown graphically again in this section in order to observe which PID provides more efficient results.

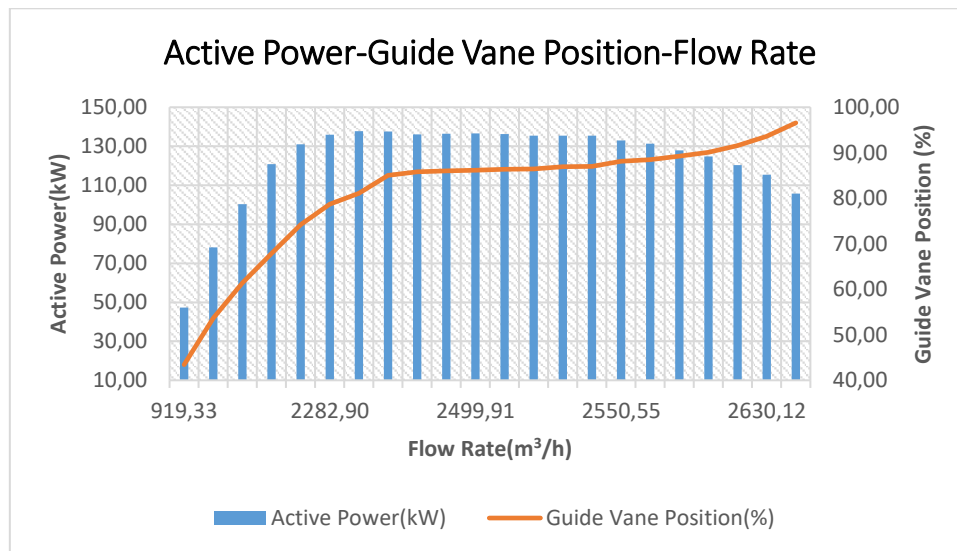


**Figure 11.** According to The Power Set PID Control Block; The Graph of The Active Power, Guide Vane Position and Flow Rate

After the system is synchronized, the requested power value is entered on the SCADA screen. Since the initial power value of the system was previously defined as 50 kW, when an energy request over 50 kW is requested, the opening percentage of the guide vane position will be increased and thus the amount of water entering the system will increase and the desired power will be obtained. At the requested power below 50kW, the percentage of the guide vane position will be reduced.

As shown in Figure 11, it is observed that when 50 kW active power is produced in the system, the guide vane position is 43% and the flow rate is 919.33 m³/h. When the power demand was increased and 100 kW active power was requested, the guide vane position was opened by 61%, thus allowing more water to pass through the system, the flow rate reached 1631.86 m³/h and the active power reached 100.36 kW. At 135 kW power demand, the guide vane position tended to remain stable at 85-86% levels, the flow rate reached between 2,499.91-2,550.55 m³/h, and the active power reached between 120.75-130.94 kW. However, when a power demand over 140 kW was requested, the guide vane position tended to open towards 100%, the guide vane did not remain in a stable position, and the amount of water passing through the system increased to 2630.12 m³/h in proportion to this opening, and the system tried

to meet this energy demand. Instantly, the active power value was observed as 137 kW and then the active power started to decrease over time, and 115 kW active power was obtained when the guide vane position was 93.63%.

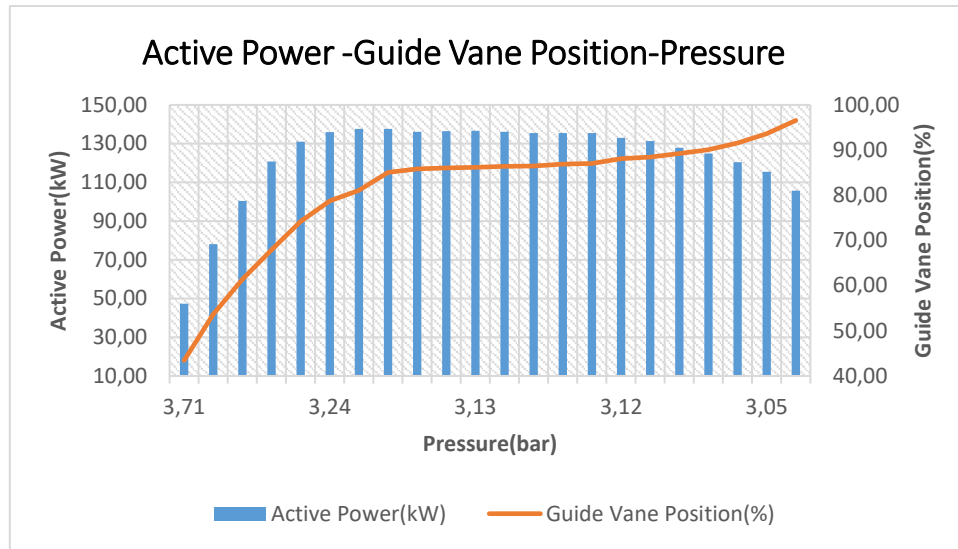


**Figure 12.** According to The Power Set PID Control Block; The Graph of The Active Power, Guide Vane Position and Pressure

As the demand power increases, the opening of the guide vane will also increase. In Figure 12, the changes in the position of the guide vane according to the demand power are graphed. At 50 kW power, the guide vane position was measured as 43% and the pressure was measured as 3.71 bar. When the demand power increased and 100 kW was produced, the guide vane position was opened by 61% and the pressure was measured as 3.54 bar. At 135 kW power demand, the guide vane position of the system tended to remain stable at 85%-86%, and the pressure value remained constant at 3.12-3.13. However, in order to meet the system demand over 140 kW, the guide vane position tended to open towards 100%, the guide vane did not remain in a stable position, the pressure dropped to 3.05 bar, and the system could not meet the requested energy.

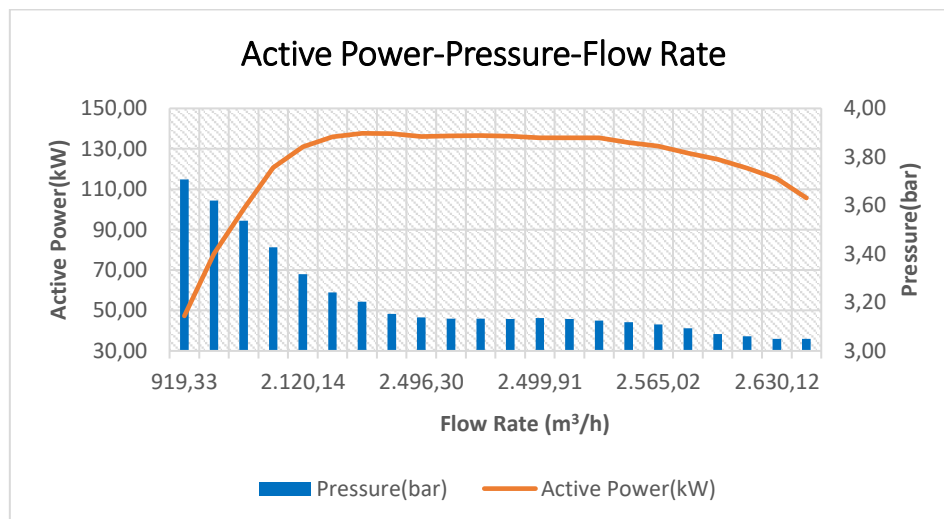


**Figure 13.** According to The Power Set PID Control Block; The Graph of The Active Power, Pressure and Flow Rate

In order to examine the effect of flow and pressure on the produced active power, the graph created according to the power set PID control is shown in Figure 13. At a power of 50 kW, the flow rate was

measured as 919.33 m<sup>3</sup>/h and the pressure was measured as 3.71 bar. When 100 kW power was requested, the flow rate increased to 1,631.86 m<sup>3</sup>/h, while the pressure decreased to 3.54 bar. When 135 kW power was requested, it increased up to 2,496.30 m<sup>3</sup>/h and started to remain stable around 2500 m<sup>3</sup>/h, the pressure maintained its balance at 3.13-3.14 bar. When the power demand was over 140 kW, more water passed through the system to provide this power, a flow rate of around 2,630 m<sup>3</sup>/h was observed, and the pressure tended to drop to 3.05-3.06 bar levels.

## **IV. CONCLUSION**

The active power and system stability studies produced by two different software, guide vane PID control and Power set PID controls, were made comparatively in this study. In the system; voltage, current, active power, pressure after the inlet valve, guide vane position, generator number of revolutions and flow rate data can be obtained from the field. However, in our study, this two different software were compared, with active power, guide vane position, flow rate and pressure values graphed.

In Figure 6, which contains the data obtained from the guide vane PID software, and in Figure 11, which contains the data obtained from the Power Set PID software, in both cases, the guide vane position initially increased linearly at the opening position to supply the required power, thus water inflow into the turbine also increased.

It is observed that the guide vane position remains stable at 87.4% and the flow rate between 2,615-2,622 m<sup>3</sup>/h in Figure 6. However, in Figure 11, the guide vane position remained stable at 85-86% for a while, and as the power demand increased, the opening ratio of the guide vane position continued to increase and showed a tendency to increase up to 100% opening ratio. However, it did not tend to remain stable at the ideal position opening. Depending on the opening position, the amount of water entering the turbine increased linearly and the flow rate increased up to 2687 m<sup>3</sup>/h.

The flow rate increased in both PID software, reaching 2,622 m<sup>3</sup>/h when examined in Figure 6, while in Figure 11 it reached 2,690 m<sup>3</sup>/h due to the 100% opening of the guide vane.

The pressure value showed the same decreasing tendency in both PID software. The pressure value, which initially started at 3.71 bar, decreased over time and remained stable at 3.11-3.12 bar in Figure 8, where the guide vane PID was applied, but in Figure 13, where the power set PID was applied, the pressure started at 3.71 bar over time. It decreased to 3.05 levels and could not maintain its stable state. We compared both software based on active power, as shown in the Figure for the guide vane PID software as observed in Figures 6, 7 and 8, a maximum active power of 137 kW was achieved and maintained. However, when observed in Figure 11, 12 and 13 in the power set PID software, the maximum active power was observed as 137 kW, but the system could not maintain constant power and it was observed that the active power decreased to 105 kW.

When the results of both software are compared, it is observed that the system works more efficiently with the guide vane PID software.

By observing the decrease in the active power value in the guide vane PID software, the guide vane position can be kept constant at the requested value. Thus, the system can be operated at its maximum power efficiency point.

Another benefit of the guide vane PID is water needs in treatment facilities periodically and hourly according to the instant demands of end users. The capacity of the treatment system is provided by water treatment up to the requested amount. Getting the requested m<sup>3</sup>/h amount of water into the system is also possible with the guide vane control. The other method is focused on the generated power and thus, flow control remains in the background and harms of the treatment plant. For these reasons, the guide vane PID control is more suitable than the power set PID control.

To enhance energy production efficiency, mitigate malfunction risks, and minimize environmental impact, future work on this project can be expanded by leveraging advancements in technology and industrial innovations. Potential areas for future research may include the following;

- Fuzzy Logic-based control strategies may be employed as an alternative to PID control, particularly in systems characterized by uncertainty and complexity.
- By utilizing big data technologies, long-term system data can be collected and processed through artificial intelligence (AI) algorithms, thereby facilitating the development of a more precise maintenance strategy.
- Optimization algorithms may be employed to enhance the energy efficiency of both the transmission line and the hydroelectric power plant. Through continuous monitoring and optimization of system parameters, improved efficiency in energy production can be realized.
- By implementing a system integrated with machine learning algorithms, predictive maintenance strategies can be developed. This system mitigates the risk of malfunctions by forecasting the optimal time for maintenance interventions.
- Through continuous monitoring using various sensors in the transmission line and power plant, deviations in parameters such as temperature, pressure, and flow rate beyond specified thresholds can be detected in advance.

**ACKNOWLEDGEMENTS:** This project was designed at the entrance of the drinking water treatment plant within the scope of "Compact and Smart HEPP Application for Facilities with Hydraulic Potential (Water Pipelines)" between TEMSAN (Türkiye Electro Mechanic Industry Corporation) Research & Design and Innovation Directorate and Metropolitan Zonguldak Union of Municipalities Administration. I would like to acknowledge and express my sincere appreciation to my esteemed colleagues who contributed to the project.

I would also like to thankfull appreciation to my supervisor Assoc. Prof.Dr. Ahmet AKTAŞ, who guided the study and my family for their moral support.

## **V. REFERENCES**

- [1] S. Virley and Dr. R. Debarre, "Energy institute statistical review of world energy report," Energy Institute, London, United Kingdom. ISSN 2976-7857, 2024.
- [2] Enerji ve Tabii Kaynaklar Bakanlığı. (2024, 24 Ekim). *Bilgi merkezi elektrik* [Çevrimiçi]. Erişim: <https://enerji.gov.tr/bilgi-merkezi-enerji-elektrik>.
- [3] A. Akpınar, M. İ. Kömürcü, M. Kankal and M. H. Filiz, "Çoruh havzasındaki küçük hidroelektrik santrallerin durumu," *V. Yenilenebilir Enerji Kaynakları Sempozyumu*, Türkiye, 2009, ss. 249-254.
- [4] N. Sanampudi and P. Kanakasabapathy, "Integrated voltage control and frequency regulation for stand-alone micro-hydro power plant," *Materialstodays Proceedings*, vol. 46, no. 10, pp. 5027-5031, 2020.



- [5] S. V. Kamble and S. M. Akolkar, "Load frequency control of micro hydro power plant using fuzzy logic controller," *International Conference on Power, Control, Signals and Instrumentation Engineering (ICPCSI)*, India, 2017, pp. 1783-1787.
- [6] Y. Oğuz, A. Kaysal and K. Kaysal, "Adıgüzel Hydroelectric Power Plant Modeling and Load-Frequency Control," *Academic Platform Journal of Engineering and Smart Systems*, vol. 3, no.1, pp. 34-41, 2015.
- [7] D. Öztürk and M. T. Özdemir, "Çok küçük güçlü hidroelektrik santrallerde PLC ile gerilim ve frekans kontrolü," *V. Ulusal Temiz Enerji Sempozyumu*, Türkiye, 2004, ss.124-130.
- [8] Ö. Polat, M. C. Bulut, İ. Dönmez and K. Özsoy, "PLC ve SCADA entegrasyonlu hidroelektrik santralin prototip tasarımı, imalatı ve 3B yazıcı ile türbin üretimi," *Adıyaman Üniversitesi Mühendislik Bilimleri Dergisi*, c.8, s.1, ss. 253-267, 2021.
- [9] A. Dalcalı, E. Çelik ve S. Arslan, "Mikro ve mini hidroelektrik santralleri için mikrodenetleyici tabanlı bir elektronik governor sisteminin tasarımı," *Erciyes Üniversitesi Fen Bilimleri Enstitüsü Dergisi*, c. 28, s. 2, ss. 1012-2354, 2012.
- [10] F. M. Ulu and H. Altınkaya, "Design, control and automation of MHPP- an experimental," *Gazi University Journal of Science*, vol. 10, no. 4, pp. 1083-1097, 2022.
- [11] C. Thanajitr, S. Polmai and S. Kittiratsatcha, "Development of Converter and Control System for Variable Speed Permanent Magnet Synchronous Generator in Small Hydro Power Plant Model," *25th International Conference on Electrical Machines and Systems (ICEMS)*, Chiang Mai, Thailand, 2022, pp. 1117-1121.
- [12] H. Kurt, "Küçük ölçekli hidroelektrik santralde bulanık mantık algoritmali PLC ile türbin kontrolü," Yüksek Lisans Tezi, Elektrik Elektronik Mühendisliği Ana Bilim Dalı, Dumlupınar Üniversitesi, Kütahya, Türkiye, 2013.
- [13] B. Yılmaz, "Özgül hız değerine bağlı olarak francis tipi türbin çarkı tasarımı ve performansının analizi," Yüksek Lisans Tezi, Enerji Sistemleri Mühendisliği Ana Bilim Dalı, Gazi Üniversitesi, Ankara, Türkiye, 2024.
- [14] B. Kudal, "İsale hatları üzerine mikro HES kurularak enerji üretimi: Bolu İli örneği," Yüksek Lisans Tezi, Bolu Abant İzzet Baysal Üniversitesi, Bolu, Türkiye, 2022.
- [15] K. Korkmaz, "Jeneratör seçim kriterleri," *II. Elektrik Tesisat Ulusal Kongresi*, Türkiye, 2009, ss. 150-160.
- [16] M. Karayel, "Mikrotip hidroelektrik santraller için PLC tabanlı SCADA sistem otomasyonu ve RTU/PLC ile frekans ve gerilim regülasyonunun gerçekleştirilmesi," Yüksek Lisans Tezi, Elektrik Eğitimi, Gazi Üniversitesi, Ankara, 2013.
- [17] Y. Aslan, C. Yaşar and M. Ç. Karabörk, "Bir mikro-hidro örneği: Kayaboğazı barajı," *Eleco Elektrik-Elektronik-Bilgisayar Mühendisliği Sempozyumu*, Türkiye, 2004, ss. 100-105.
- [18] O. Bendeş, B. Yılmaz, F. Koç and A. Yıldız, "Banki türbini verimlilik artışı için tasarım parametrelerinin sayısal ve deneysel olarak incelenmesi," *Dicle Üniversitesi Fen Bilimleri Enstitüsü Dergisi*, c. 12, s. 1, ss. 448-64, 2023.
- [19] W.Ali, H.Farooq, M.Usama and A.Bashir, "PID vs PI control of speed governor for synchronous generator based grid connected micro hydro power plant," *Journal of Faculty of Engineering Technology*, vol. 24, no. 1, pp. 53-62, 2017.

[20] Siemens Industry Online Support. (2024, 18 August) *PID control with PID compact for SIMATIC S7-1200/S7*. [Online]. Available: [https://support.industry.siemens.com/cs/document/100746401/pid-control-with-pid\\_compact-for-simatic-s7-1200-s7-1500?dti=0&lc=en-WW](https://support.industry.siemens.com/cs/document/100746401/pid-control-with-pid_compact-for-simatic-s7-1200-s7-1500?dti=0&lc=en-WW).

[21] S. Kaçar, A. F. Boz, B. Aricioğlu and H. Tekin, “PID denetleyici uygulamaları için yeni bir online deney seti tasarımı,” *Journal of Sakarya University Institute of Science and Technology*, c. 21, s. 1, ss. 1-13, 2016.